Journal of Energy Storage

Simplified modelling of nonlinear electromethanogenesis stack for power-to-gas applications

Mahdi Shahparasti[a,c,*], Salim Bouchakour[a], Alvaro Luna[a], Daniele Molognoni[b], Pau Bosch-Jimenez[b], Eduard Borràs[b]

[a] Department of Electrical Engineering, Technical University of Catalonia, 08222 Terrassa, Spain
[b] LEITAT Technological Center, C/ de la Innovació 2, 08225 Terrassa, Spain
[c] Electrical Engineering Section, The Mads Clausen Institute, University of Southern Denmark, 5230 Odense, Denmark

ARTICLE INFO

Keywords:
Bioelectrochemical system
Electromethanogenesis
Equivalent circuit model
Non-linear behaviour
Parameter estimation
Power-to-gas

ABSTRACT

Bioelectrochemical systems performing electromethanogenesis (EMG-BES) represent an emerging technology for Power-to-gas as well as wastewater treatment. Moreover, EMG-BES can be used as a high-capacity energy storage system to absorb surplus energy in the electrical grid. This paper presents a modelling approach, which is based on building an equivalent electric circuit of the EMG-BES, which can be used to emulate static and dynamic non-linear behaviour of EMG-BES for different input voltages, which is advantageous if compared to other existing models. This model is a suitable choice for future studies in the development of the electric converters for EMG-BES plants connected to the electrical grid. The proposed model consists of practical and commercial elements, including capacitors, resistors, voltage sources, and a diode. The modelling of non-linear behaviour is achieved by adding a diode to the model. Four simple tests were performed to determine the equivalent circuit parameters in a medium-scale EMG-BES prototype. This prototype was built by stacking 45 cells together and connecting them in parallel, and it was long-term operated and tested under different electric inputs to determine the model parameters. A comparative study was finally conducted as reported in this paper in order to validate the proposed model against experimental results and values collected with other models.

1. Introduction

In the electric power sector, energy storage systems are claimed to play a decisive role in order to overcome issues like the lack of balance between power fluctuations and energy demand in electrical energy grids, specifically to deal with their temporal component [1–3]. Depending on the time scale, there are different roles that storage can play [4,5], as well as different technologies. Nowadays, different available technologies (e.g., supercapacitors, batteries) allow short-term energy storage and fast power dynamics, but they are characterised by a limited capacity [6,7]. On the other hand, pumped hydro or compressed air storage are good candidates for large-scale storage, but they require large investment costs and significant construction efforts [8–10]. The power-to-gas (P2G) technology is an attractive alternative that can contribute to the conversion of a high amounts of surplus electric energy from renewable energy resources into more easily storable gaseous fuels, like H_2 or synthetic natural gas (SNG) [11,12]. In the latter case, the P2G technology aims at the production of SNG, containing CH_4 as a major component [13]. This SNG can be injected into the natural gas grid or directly used as vehicle fuel [3,14]. Storing energy in the shape of methane permits to provide an alternative to overexploited electrochemical batteries (Li-ion, lead-acid, etc.), especially for large-scale storage applications, resulting in a more stable and flexible power system [15]. The interconnection of gas and electrical networks gives rise to almost unlimited storage capacity, linking two existing large-scale infrastructures already available [16]. A recent modelling study showed that the utilisation of P2G as energy storage facility could reduce the levelised cost of energy in energy systems with a high share of intermittent renewable energy sources [13] Furthermore, for each CH_4 molecule produced, a CO_2 molecule is consumed, reducing the climate impact of burning natural gas and moving forward towards a circular economy concept [15]. Moreover, the production of CH_4 from renewable energy and CO_2 will allow decreasing EU dependence from fossil fuels importation, accelerating the decarbonisation of industrial, residential and transport sectors [17].

At the present time, chemical and biological methanation are the two industrial processes available for P2G installations [18], both requiring an external H_2 source for the subsequent reduction of CO_2 to

* Corresponding author at: Electrical Engineering Section, The Mads Clausen Institute, University of Southern Denmark, 5230 Odense, Denmark.
E-mail address: mshah@mci.sdu.dk (M. Shahparasti).

CH_4. This H_2 is generally produced by water electrolysis [19]. Among the available electrolysis types, the alkaline electrolysis was the first one to be developed and is nowadays a mature technology, showing a competitive costs [20]. However, its H_2 production efficiency (63–70%) and response speed is limited (1–10 min) [21]. Proton exchange membrane (PEM) electrolysis shows higher response speed (seconds to minutes), higher current density and H_2 purity than alkaline technology, although at higher costs and lower efficiencies (50–60%) [21]. High-temperature electrolysis is the newest technology, showing the highest energy conversion kinetics and efficiency (74–81%) but is the less mature technology, only demonstrated at laboratory and small demonstration scale [22]. Moreover, it shows high CAPEX cost and the operation at high temperature (650–1000 °C) limits its applicability.

An alternative P2G technology is under development, based on bioelectrochemical systems for electromethanogenesis (EMG-BES) [23]. In this case, wastewater treatment is coupled with CO_2 conversion to CH_4 by means of bioelectrochemical systems [24]. Therefore, EMG-BES technology can connect electric, wastewater and natural gas grids, reducing the overall energy cost and improving the overall system resiliency.

Moreover, EMG-BES has several potential advantages compared to previously mentioned methanation technologies. In addition to be a single step process, not requiring preliminary H_2 production, it can occur at mild temperature and pressure (25–35 °C, atmospheric pressure) [25]. This can potentially reduce the operational costs without affecting the quality of generated biomethane. However, this technology is nowadays in its early stage of development, and achievable CH_4 production rates are still low compared to the other methanation technologies [23]. A few attempts of scaling-up EMG-BES reactors were reported in the literature [26,27], demonstrating that the technology is not yet ready to be industrialised. Among others, scaling up these systems involves the development of different aspects, including (1) reactor architecture and electrodes materials, which should improve current density and reactions rate, (2) control and monitoring of input wastewater and output effluent, (3) injection of produced methane into the natural gas grid, (4) electric control system for linking the EMG-BES plant to the electric grid. In this regard, the use of an electric converter, as shown in Fig. 1, is required to connect EMG-BES to the electrical grid because its input voltage is direct current (DC) while the grid is alternating current (AC) [28]. The converter must convert the AC input voltage to a variable DC voltage. Then, the amount of electric power converted to CH_4 as well as the level of wastewater treatment are controlled by changing the input voltage of the EMG-BES system, using the converter [29]. Several topologies including single-stage single-output and multi-stage multi-output AC/DC converters have been proposed for interlinking stacks and the electrical grid [25,28,30,31]. For designing this converter, it is mandatory to have an accurate electric model, able to cover the static and dynamic behaviour of EMG-BES cells for different operation modes [32]. Moreover, this model must be implementable using practical electrical elements. This is one of the main aims of this paper as few contribution are available in the literature, and none related to control strategies for electric converters under a changing input power.

In general, there are two approaches to model BES. On the one hand, the knowledge of microbiology and bioelectrochemistry can be used to characterise the cell behaviour [33]. On the other hand, the electrical equivalent circuit (EEC) modelling method can emulate the reactor as an electrical circuit to represent fast electrical processes, while neglecting the relatively slow dynamics of biomass metabolism and growth [34]. It was demonstrated in [35] that electrical circuit models of a microbial fuel cell (MFC) could be used to adequately describe the dynamics of an EMG-BES system, as both of them share the same anodic bioreactions. Both MFC and EMG-BES are complex and hybrid systems involving several bioelectrochemical coupling reactions, which leads to strong non-linear characteristics and significant hysteresis properties.

In bioelectrochemical systems, electrical charge is accumulated at the interface layer between the bioelectrode and the electrolyte, thus a step change of voltage results in a fast change of current traced by a slow transition towards equilibrium [36]. BES electrodes work as a biological supercapacitor, enabling thus to store energy and to perform a fast delivery of electrical charge. A common and straightforward way to model the double layer capacitance is an EEC with the charge storage represented by an electrical capacitor [35].

On the other hand, the electrochemical impedance spectroscopy approach was proposed to illustrate polymer electrolyte membrane fuel cells using an EEC with a resistance (R) and a capacitor (C) [37,38]. These processes are emulated by connecting those elements in parallel or series. A similar method was proposed for MFC by Ramasamy et al. [39] to study the biofilm growth impact on the anode impedance, as well as to determine the internal resistance, as shown in [40]. The parallel connection of a resistor and a capacitor (R–C) was adopted to represent the charge transfer resistance and the double layer capacitance effect. A resistance connected in series with the R–C element represents the ohmic resistance of the electrolytes and the membrane. Adding more R–C branches to the basic circuit allowed a more detailed description of the MFC dynamic activities. To solve the drawbacks of the conventional EEC with parallel R–C branches for simulating the

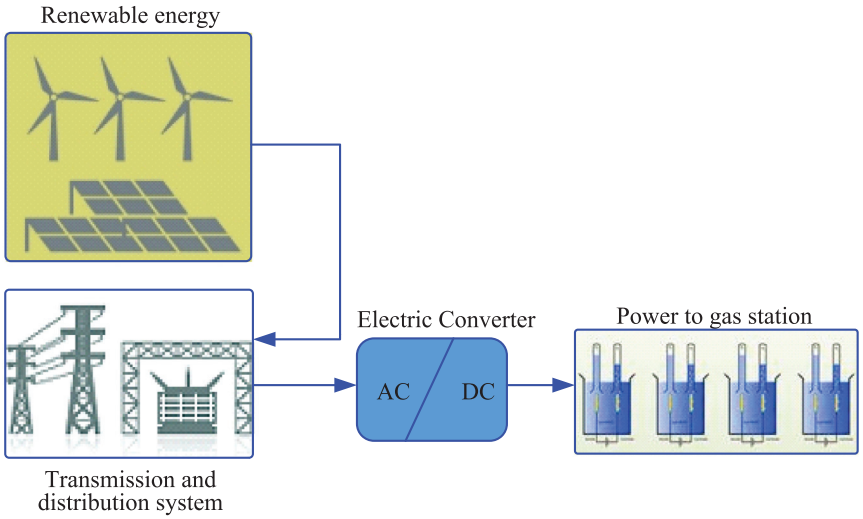

Fig. 1. Schematic of power to gas energy storage.

behaviour of the discharge in the double-layer capacitor, the work in [41] proposed an EEC which had advantages in describing the anodic electron flow and electric charge storage behaviour of an MFC system. The proposed model in [41] used an equivalent capacitance in parallel and a series resistances to accurately model MFC. The work published in [42] proposed an EEC based on parallel R–C branches for microbial electrolysis cell (MEC) operation and introduced a parameter estimation procedure for real-time monitoring.

Nevertheless, all these contributions are not able to cover the modelling completely. In a nutshell, EEC models use linear elements such as resistors and capacitors to describe BES cells; therefore, they cannot model any non-linear current–voltage characteristics. The accuracy of the model is vital for designing a power management system for the EMG-BES system.

In order to overcome these drawbacks this study presents a new modelling of a medium-scale BES prototype for methane production and electricity storage. A series of electric characterisation tests are performed to model the prototype electric behaviour and to design a converter for grid integration of EMG-BES systems. A new electrical model with one resistor–voltage (R–E) branch and one diode–resistor–voltage (D–R–E) branch is proposed to model EMG-BES non-linearity. The obtained results are compared with experimental results and typical electrical models to verify its performance.

This paper is organised in 5 sections. Section 2.1 explains the construction of the proposed EMG-BES stack. Recommended electrical tests for modelling are described in Sections 2.2 and 2.3, respectively. Then, the proposed electrical model is compared with typical methods in Sections 3 and 4. Finally, conclusions are covered in Section 5.

2. Material and methods

2.1. EMG-BES prototype characterisation

A medium-scale EMG-BES prototype was built by connecting in parallel 45 cells together, grouped by 3 into 15 single-chamber, membrane-less reactor modules. The volume of each reactor module and the total prototype capacity were 1.78 L and 32 L, respectively. Anode and cathode electrodes (0,77 m^2 each one) were made of thermally activated carbon felt (SGL Group, Germany). Stainless steel current collectors made the electric connection to the external circuit. The complete stack was electrically connected in parallel and powered at 0.7 V by an external power source (TENMA 72-2715, Farnell, Spain). The produced gas in the prototype was trapped by three external chambers, each one connected to 5 reactor modules (gas traps in Fig. 2). The reactor modules were hydraulically connected in parallel, maintained at a constant temperature of 25 °C and continuously fed with 10 L d^{-1} of municipal wastewater (collected at the local treatment plant), as detailed in [26].

The current (I) consumed by each cell was calculated using a shunt resistor of 4.8 Ω, installed in series with each cell. Three 16-channels DAQ boards (PicoLog 1216, Farnell, Spain) were adopted for this purpose. The current density was obtained by dividing it by the cathode surface. The complete setup with EMG-BES stack, input power source, gas traps and data loggers for BES monitoring is shown in Fig. 2.

For using the EMG-BES stack as an electrical energy storage system, one power converter has to be interfacing the stack and the grid, because the grid voltage is AC, but the required voltage for the bioelectrochemical process is determined by DC voltage (see Fig. 1). Depending on the grid situations and the electricity price, this converter has two working modes:

1) Standby mode: In this mode, the current of EMG-BES stack is kept around zero, and there is not any power exchange with the grid. The converter goes to this mode, either if the frequency of the grid is lower than the nominal value or the electricity price is high.
2) Power mode: The converter switches to this mode when the grid price is low, or the EMG-BES stack is going to work in frequency support mode in grid over-frequency case. In this mode, the converter applies a variable and regulated voltage to the stack for adjusting the value of exchanged power with the grid.

For designing this converter, the electrical behaviour of the EMG-BES stack in steady-state and dynamic situations has to be determined.

2.2. Electric characterisation

Four electrical tests have been performed to explore the behaviour of the stack:

1) Constant voltage test: This test is done in order to determine the behaviour of the stack in steady-state under nominal voltage.
2) Short circuit test: Feeding the stack with a pulse modulated wave shape voltage is one option to supply it with variable voltage, in which voltage toggles between zero and a specific value. Zero voltage equals to short circuit condition (SC); hence, this test is useful to determine the behaviour of the stack in SC State. Also, the test

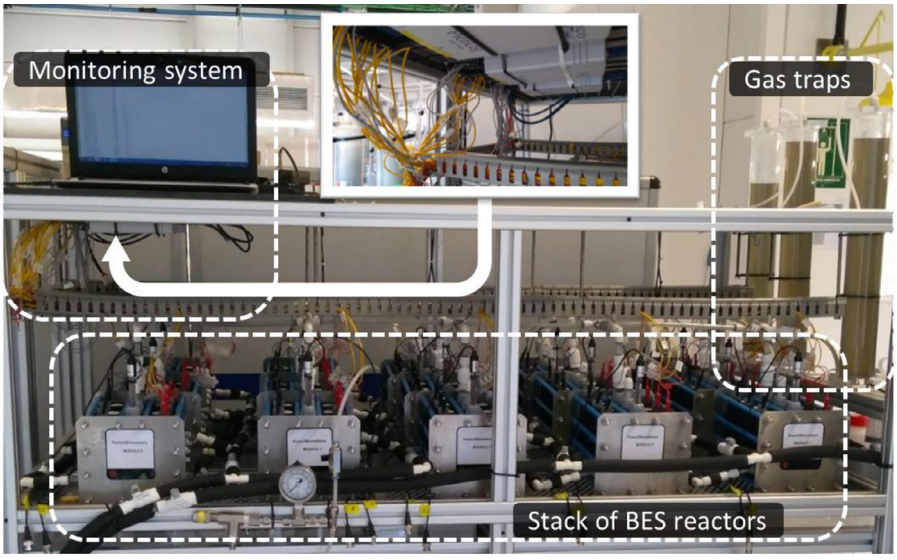

Fig. 2. Stack of reactor modules composing the EMG-BES prototype.

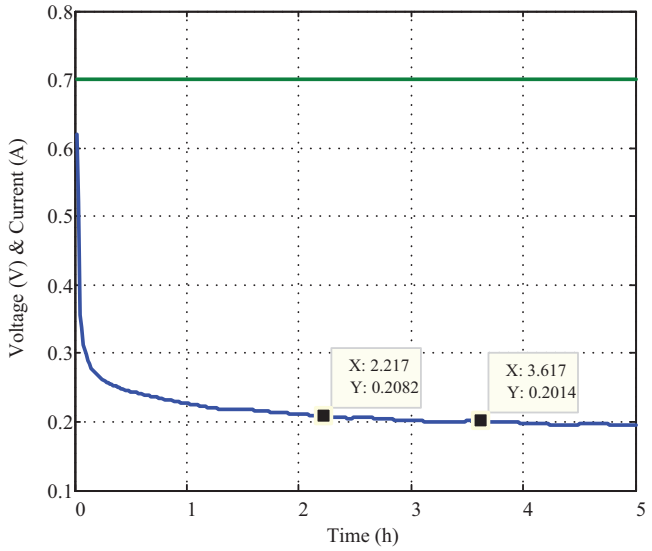

Fig. 3. Experimental result: constant voltage test.

will be used to find the value of a single equivalent capacitance in electrical models.

3) I–V curve: The test is useful to determine the static and dynamic behaviour of the EMG-BES stack for different levels of the input voltage. An I–V (current–voltage) curve measurement is accomplished by applying a series of voltages to the stack.
4) Voltage step test: A voltage step test is used to determine the dynamic behaviour of the stack. The voltage changes between the two specified values as quickly as possible, and the current waveform is captured.

2.2.1. Constant voltage test

Before analysing the I–V curve, a preliminary test should be done to know the time needed by the prototype to stabilise on a new voltage level. The test was conducted varying the applied voltage from open circuit to 0.7 V and measuring the current (every 10 s). The obtained result is shown in Fig. 3, where it can be seen that the settling time of the current response is around 2.3 h.

2.2.2. Short circuit test

A short circuit test is done by imposing a voltage of 0 V to the prototype. The test lasted 30 min, and the current was measured every 0.1 s. Negative transient current peaked at −2.5 A, due to the short sampling time (Fig. 4). The current stabilised on a negative value as the applied voltage was lower than the open-circuit voltage (OCV), i.e. electrons were flowing from the cathode to the anode of the system.

2.2.3. I–V curve

The I–V curve test is obtained using the potentiostat (SP-150, BioLogic). The current was measured every 2 min. The obtained results for the electrical characterisation of EMG-BES stack is shown in Fig. 5 in which there are four working areas: In area 1, the current of the stack is maintained around zero with applying 0.115 V to stack. This means that the real converter has to apply a minimum voltage in standby mode to prevent the current circulation. In area 2, when the input voltage reduces to zero, the direction of the current is reversed. This area is a forbidden area, and the electric converter has to avoid reverse current with supplying stack continuously with a minimum voltage. In area 3, the value of stack current changes corresponding to the amplitude of the applied voltage. The converter has to control the stack voltage in this voltage range, when it is working in power mode. Area 4 represents the saturation stage for the stack (voltage higher than 1 V). The value of the current is almost constant, and the stack becomes unstable while the

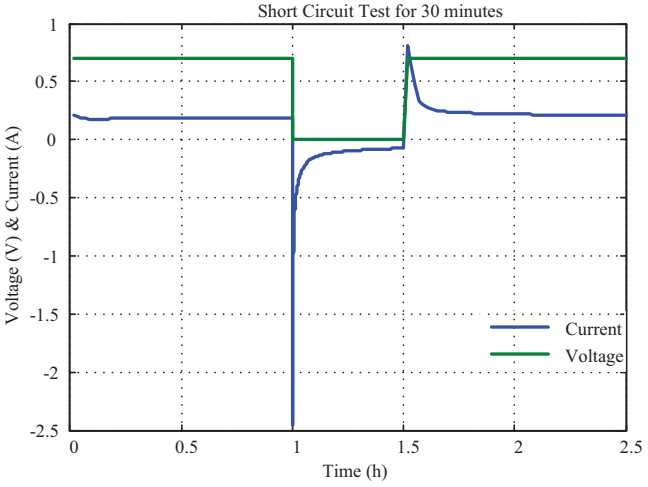

Fig. 4. Experimental result: short circuit test.

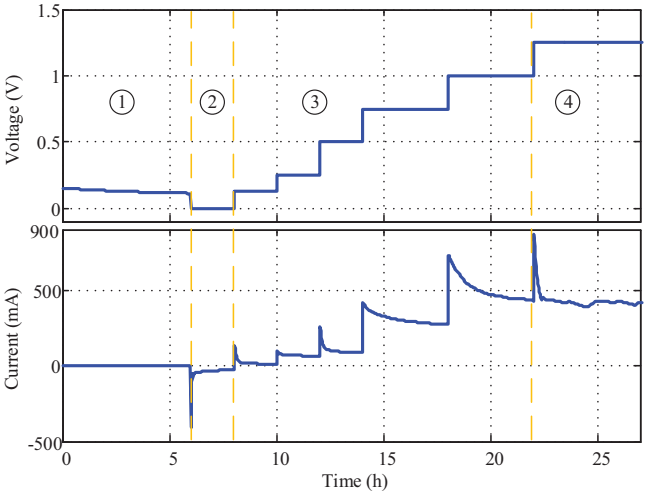

Fig. 5. Experimental result: current–voltage curve test.

applied voltage increases. Thus, the converter must not enter this area.

2.2.4. Step voltage test

Several operation tests were performed with a potentiostat, varying the applied voltage from its nominal value to OCV, at different duty cycles. The current consumption was measured once per second. The prototype was left at the nominal voltage for 5 h between each series of tests. The current consumption was zero during the periods in OCV.

The obtained results of the two tests are shown in Fig. 6 and Fig. 7. The experimental results show that: (1) the prototype was not negatively affected by the periods in OCV, (2) current consumption at the nominal voltage (in steady-state conditions) remained around 200 mA during the whole experimental duration, (3) the peak of current for the first voltage step is the highest current during the test (around 2.15 A), then it reduces to around 1.8 A for the other voltage steps.

2.3. Chemical characterisation

The production of CH_4 in the proposed prototype is due to two factors: the electro-active bacteria, the ones storing electric energy in the chemical form, and the methanogenic microbes, by transforming the acetate content of wastewater into CH_4 without electricity consumption, therefore not contributing to electricity storage. Due to the hydraulic configuration adopted, the measurable CH_4 production rate is quite variable in time, and any significant difference can be seen only

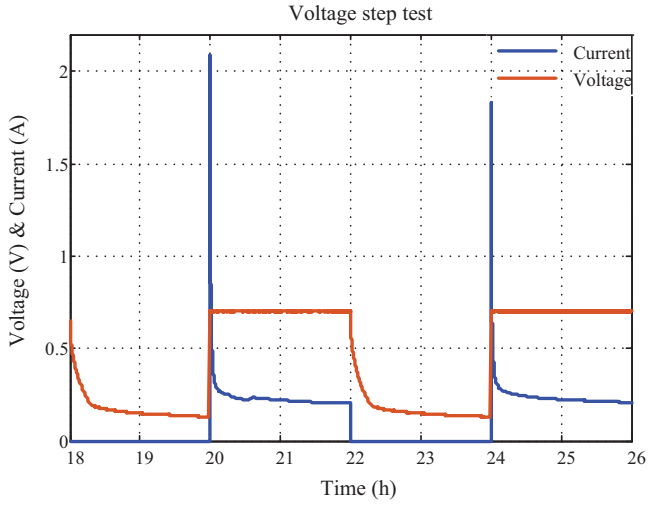

Fig. 6. Experimental result: voltage step test for the EMG-BES stack for two hours in open circuit state and two hours in nominal voltage state.

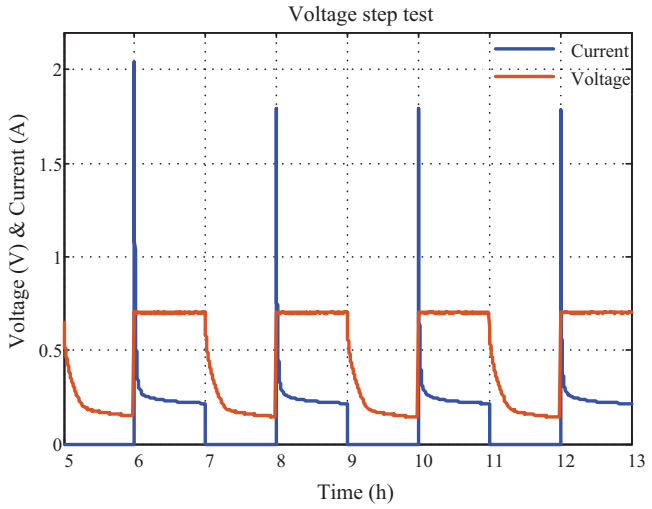

Fig. 7. Experimental result: voltage step test for EMG-BES stack for one hour in open circuit state and one hour in nominal voltage state.

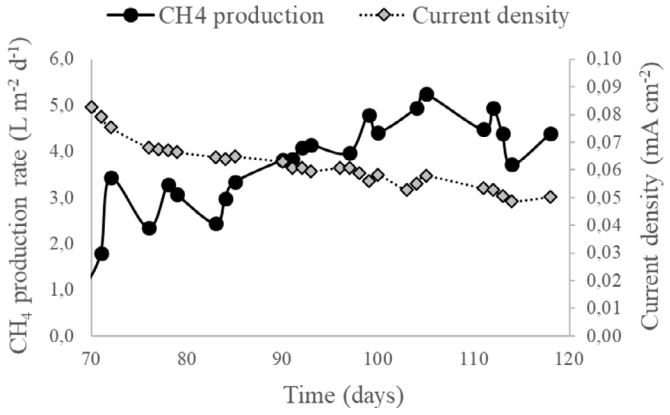

Fig. 8. Current density and CH_4 production rate in the long-term test (readapted from [12]).

with long sampling times like a week. Fig. 8 shows the current density and CH_4 production rate measured in a long-term test. It can be seen that it is impossible to find a precise relationship between the consumed current and the produced CH_4. Still, it is clear that the rate of CH4 production is positive when a voltage is applied, and it stabilises around a specific value.

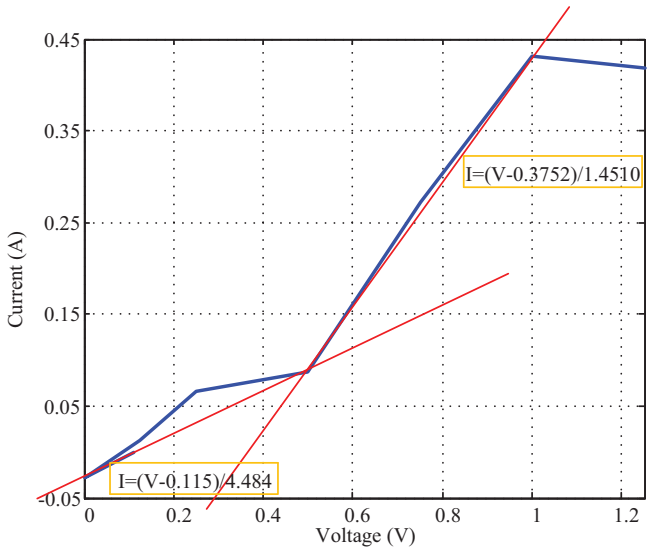

Fig. 9. The current–voltage curve for an EMG-BES stack.

3. Physical and mathematic modelling

If the current vs voltage curve of EMG-BES stack in steady-state is drawn based on I–V tests results of Section 2.2.3, then the Fig. 9 will be obtained. Feeding the stack with a voltage higher than 1 V is forbidden because the current saturation occurs, and the insulation of cells may also be threatened. Besides, the stack has to be supplied with a voltage higher than 0.115 V to avoid reverse current flow according to the open-loop test. Therefore, EMG-BES voltage should be changed between 0.115 V and 1 V. As it can be seen from these curves, the nonlinear behaviour in the steady-state can be expressed with two lines. Only one line models the behaviour between OCV and 0.5 V because the level of current is low and unpredictable in this area. Moreover, the obtained results of a real EMG-BES stack under a step voltage change showed that its dynamics can be approximated to first-order system, including resistor and capacitor.

This paper proposes a new model for modelling the EMG-BES stack depicted in Fig. 10, able to represent its dynamic behaviour as well as its non-linear characteristics in steady-state. This model has one resistor-dc source branch and one resistor-dc source-diode branch, which are connected in parallel with a capacitor, then a small resistor is installed in series with these branches. In fact, two lines are proposed for achieving a better curve fitting of the EMG-BES stack, where each branch corresponds to one line in Fig. 9. It is worth to mention that the diode in branch 2 is used to model nonlinearity and to prevent the flow of current between branches. Also, one RC circuit is considered in series with R–E branches to model the dynamic profile of EMG-BES. The real diode has a turn-on voltage drop and a forward resistance; however, it does not affect the accuracy of modelling, since a resistor and a voltage

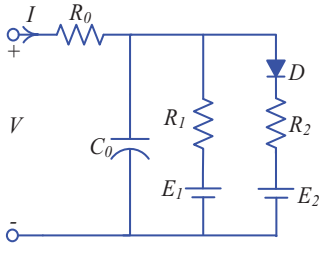

Fig. 10. The proposed dynamic model of EMG-BES stack.

source are installed in series with diode. Therefore, the internal resistor and voltage drop of the diode can be considered as part of them in Fig. 10.

The parameters of the proposed model can be mathematically obtained from real data. The value of R_0 can be found based on a startup current when R–E branches are short-circuited by capacitor C_0:

$$R_0 = \frac{V_{st}}{I_{st}}, \tag{1}$$

where V_{st} and I_{st} are voltage and current of the EMG-BES during the startup. According to Fig. 9, it has two working modes based on the value of the input voltage, which can be expressed with two lines in steady-state:

$$I = \begin{cases} \dfrac{V - A}{B} & 0 \le V \le E \\ \dfrac{V - C}{D} & E \le V \le V_{max} \end{cases} \tag{2}$$

where A, B, C, D, E, and V_{max} are constant values that can be found from the I–V curve by curve fitting in Fig. 9 as follows:

$$I = \begin{cases} \dfrac{V - 0.115}{4.484} & 0 \le V \le 0.5 \\ \dfrac{V - 0.3752}{1.4510} & 0.5 \le V \le 1 \end{cases} \tag{3}$$

Next, the values of R_1 and E_1 of the proposed model can be expressed as follows:

$$R_1 = B - R_0. \tag{4}$$

$$E_1 = A. \tag{5}$$

Then, values R_2 and E_2 can be calculated as:

$$R_2 = [(D - R_0)^{-1} - R_1^{-1}]^{-1}. \tag{6}$$

$$E_2 = (R_1^{-1} - R_2^{-1})R_2C - R_2R_1^{-1}E_1. \tag{7}$$

Finally, current in the short-circuit test can be integrated to determine the equivalent capacitance C_0 as follows [41]:

$$C_0 = \frac{1}{V_{OC}} \int i_{sc}(t)dt, \tag{8}$$

The interpretation of the proposed model and its relationship with the working principles of the EMG-BES technology will be done based on Fig. 11. The technology is based on electromethanogenesis (EMG),

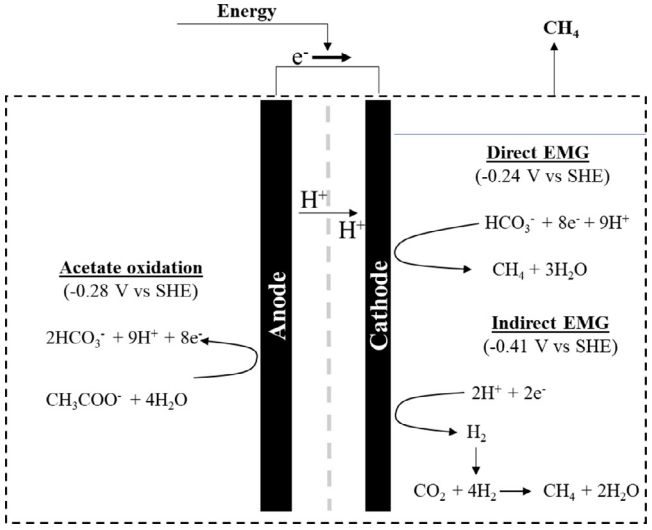

Fig. 11. Experimental result: resume of the possible reactions taking place in an MES reactor.

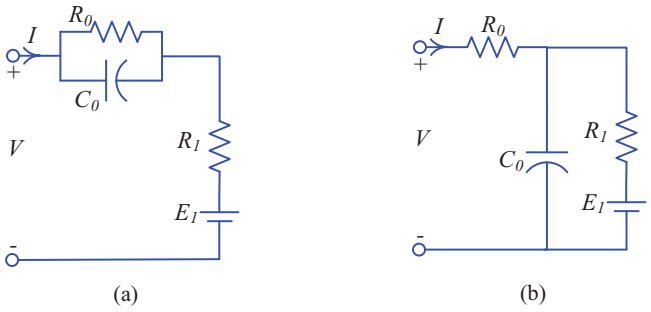

Fig. 12. Conventional dynamic model of BES, (a) Model 1 [34,43], (b) Model 2 [41].

where the cathode acts as an electron donor for the biotic reduction reaction. This can be the direct reduction of CO_2 to CH_4 (direct EMG), or the production of H_2 as an electrochemical mediator, which then reacts with CO_2 producing CH_4 (indirect EMG). These two reduction reactions take place at different reduction potentials: direct EMG at −0.24 V vs SHE, indirect EMG at −0.41 V vs. SHE (where SHE stands for standard hydrogen electrode). At the anode, the electrons are provided by the acetate oxidation due to the electro-active bacteria. As a result, two voltage levels, one about 0.2 V and another about 0.4 V are required to drive EMG reactions (direct and indirect one), which is well included in the proposed model as E_0 and E_1. Also, three resistors and one capacitor are proposed to consider ohmic and double-layer charge characteristics of EMG-BES.

4. Results and discussion

A comprehensive comparison between the proposed model and conventional models will be driven in this section of the paper in order to evaluate its efficiencies. Two typical electrical models of BES, titled model 1 [34,43] and model 2 [41], are shown in Fig. 12. Typically, the model parameters are chosen based on data of experimental tests in the nominal state. The obtained parameters for model 1 and model 2 are listed in Table 1. The parameters of models 1 and 2 are the same, and only components are connected in two different ways.

Parameters of the proposed model in Table 1 have been found from the current–voltage curve (Fig. 9) and the short circuit test.

SimPowerSystems toolbox of MATLAB software is used for comparison of models. As shown in Fig. 13, the proposed circuit and conventional dynamic models are made using electrical elements in MATLAB environment. The sample time of simulation is set 0.01 s because the simulation must be done for 8 h and smaller sample time leads to overloading of a computer with Intel Core i7 processor and 8 GB DDR3 RAM. Besides, ode23tb is used as a solver in this simulation. The obtained results, applied voltage and measured current, taken from real experiments were loaded in the simulation as *in* and *out* in Fig. 13. The applied voltage in the experimental setup is applied as the input (*in*) to all circuits, and the resulting results are captured and compared. In Fig. 13, the currents of models and experiment current (*out*) are captured at the same time.

The comparison is made based on two cases: (1) step change from open circuit state (0 V) to nominal voltage with two different duty cycles, (2) variable voltage input (I–V curve).

The comparisons between models in case of voltage step from zero

Table 1
Model parameters.

	R_0 (Ω)	C_0 (F)	R_1 (Ω)	E_1 (V)	R_2 (Ω)	E_2 (V)
Model 1	2.576	316.8	0.3193	0.115	–	–
Model 2	0.3193	316.8	2.576	0.115	–	–
Proposed	0.3193	316.8	4.1647	0.115	1.5539	0.4723

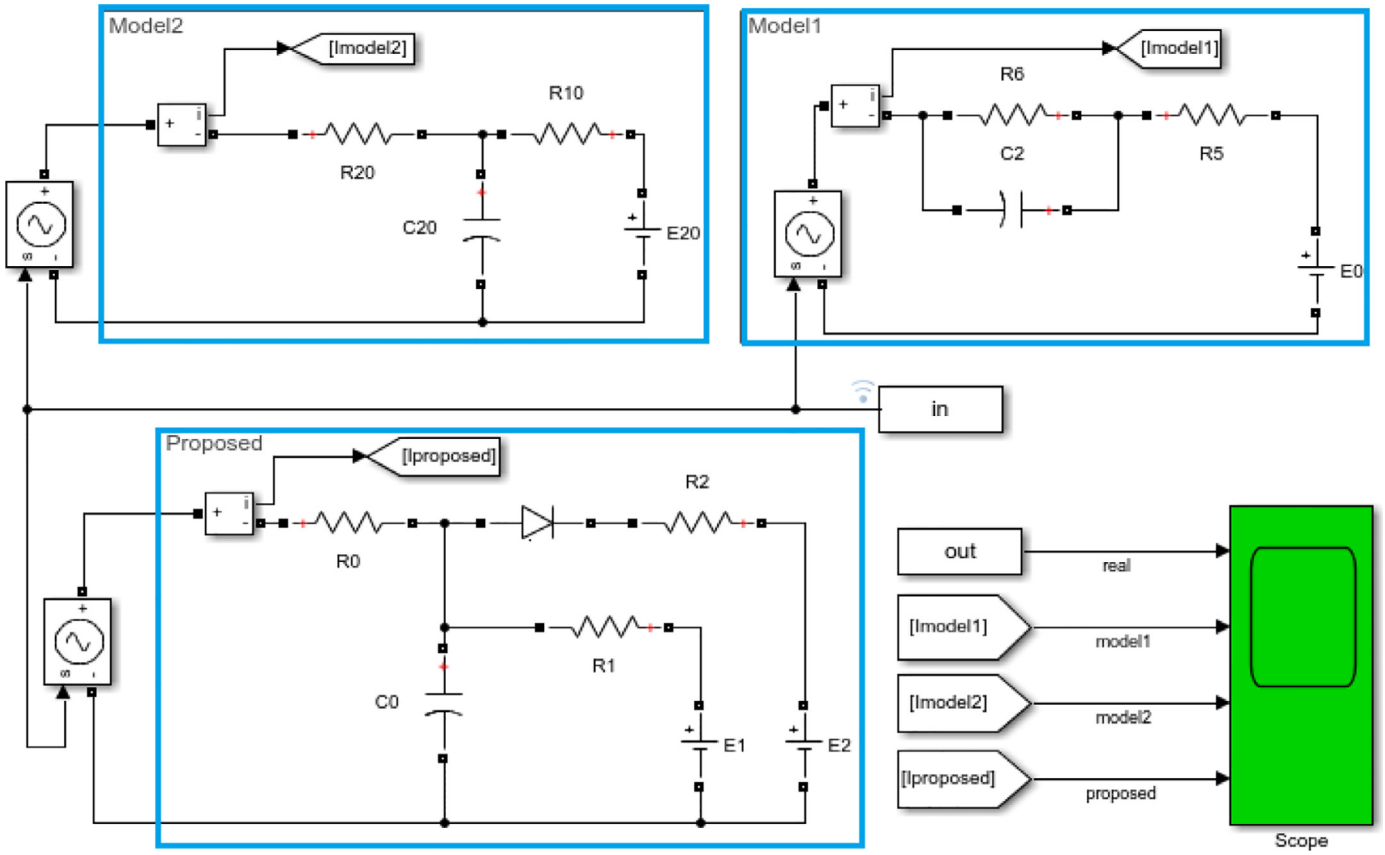

Fig. 13. MATLAB simulation circuit.

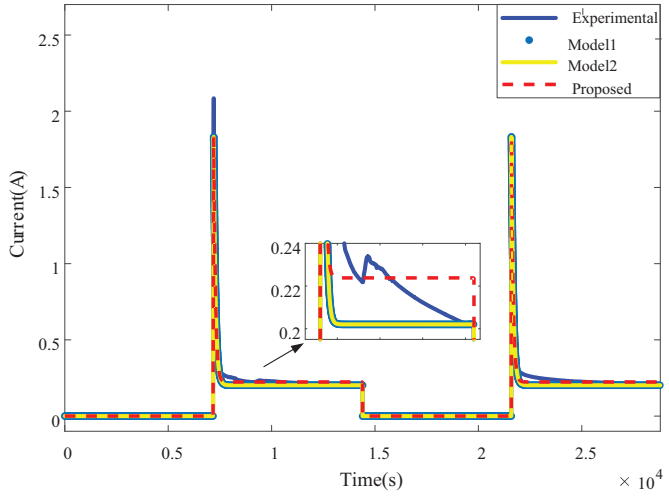

Fig. 14. Comparison of models for voltage step from open circuit (0 V) to nominal voltage in 2 h.

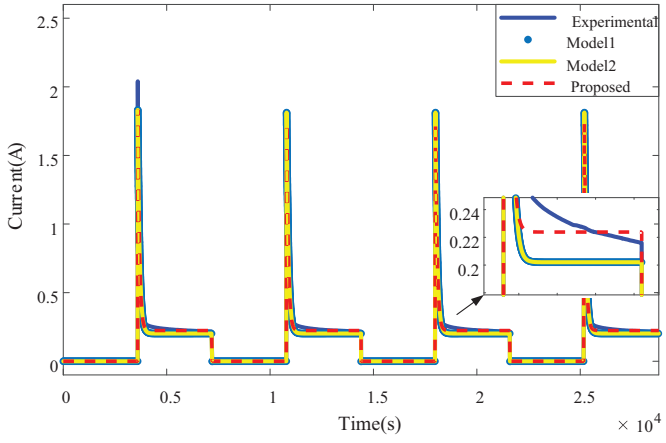

Fig. 15. Comparison of models for voltage step from open circuit (0 V) to nominal voltage in 1 h.

to nominal voltage in two different periods are shown in Fig. 14 for a duty cycle of 2 h, and in Fig. 15 for a duty cycle of 1 h. The obtained results show that models 1 and 2 and the proposed model can emulate the static and dynamic behaviour of the stack accurately for step-change to nominal voltage, and the steady-state errors of the models are less than one percent, which is acceptable accuracy. Therefore, all models work correctly at nominal voltage.

The response of the models for the current–voltage curve test is the best criterion to demonstrate the superiority of the proposed model in comparison with the conventional models because the stack has a nonlinear behaviour. A comparison of the results is presented in Fig. 16, where it can be observed that models 1 and 2 have the same response, and they cannot model the non-linear behaviour of the real stack. The inaccuracy of models 1 and 2 is more evident for operating the voltage between 0.8 V and 1 V. On the other hand, the proposed model represents the non-linear behaviour of the stack for different voltage precisely, and the error of modelling is zero in steady-state. The absolute magnitude of the differences between the experimental results and the models' outputs are shown in Fig. 17, where the results show that the proposed model has high accuracy in the modelling of the stack in both steady-state and transient state.

In summary, the obtained results show that the proposed model has more accuracy for modelling a BES with variable input voltage according to the comparison of experimental results of real EMG-BES

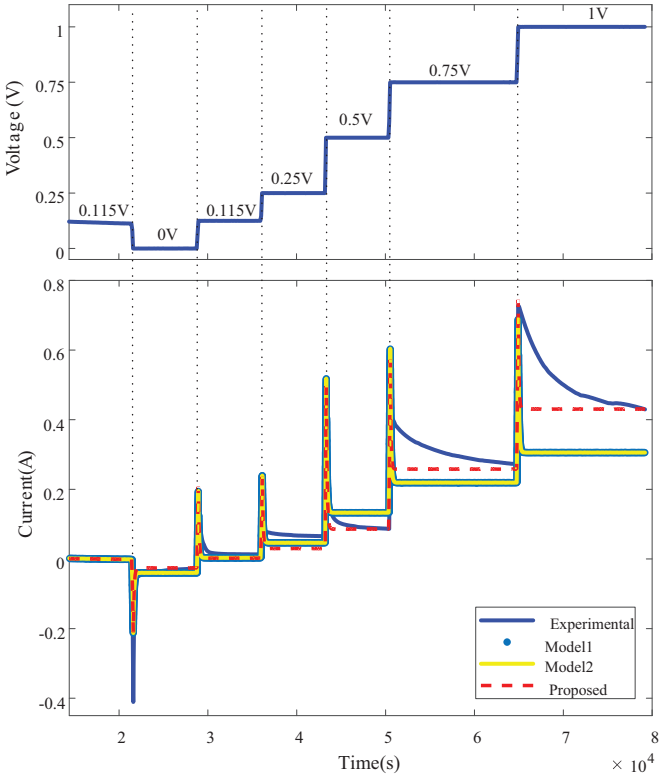

Fig. 16. Comparison of models for I–V curve: voltage and current.

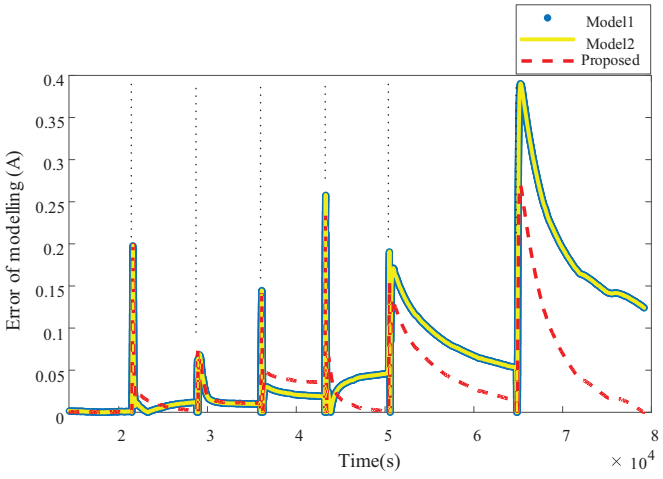

Fig. 17. Comparison of models for I–V curve: error of modelling for different models.

stack with different models.

5. Conclusions

In this paper, a new equivalent-circuit-based model for EMG-BES considering non-linear static and dynamic behaviours was proposed. The proposed equivalent circuit explains the possible internal reactions of an EMG-BES cell accurately compared to the conventional equivalent circuits with one branch. This model consists of a resistor- dc source and resistor- dc source-diode branches in parallel with a capacitor and in series with a resistor. A medium-scale EMG-BES reactor is constructed and tested with four simple test methods, fixed voltage, short circuit test, current–voltage curve, and voltage step to identify the parameters of the proposed equivalent circuit. The proposed and conventional models with real input are tested in SimPowerSystems toolbox of MATLAB software, and the obtained results verify that the proposed model has higher accuracy than the other models.

Declaration of Competing Interest

The authors declare that they have no known competing financial interests or personal relationships that could have appeared to influence the work reported in this paper.

Acknowledgements

The research leading to these results has received funding from the European Union's Horizon 2020 research and innovation programme under the Marie Skłodowska-Curie grant agreement No 712949 (TECNIOspring PLUS) and from the Agency for Business Competitiveness of the Government of Catalonia.

Also, this work has been supported by the Spanish Ministry of Economy and Competitiveness under the projects RTI2018-100921-B-C21. Any opinions, findings and conclusions or recommendations expressed in this material are those of the authors and do not necessarily reflect those of the host institutions or funders.

The authors wish to acknowledge the Leitat collaborators who took part in Power2Biomethane project, which was financially supported by the Spanish Ministry of Economy and Competitiveness (RTC-2016-5024-3, 2016).

Author statement

Mahdi Shahparasti: Investigation, Conceptualization, Methodology, Software and Writing, Salim Bouchakour: Writing, Alvaro Luna: Project administration and Supervision, Daniele Molognoni: Investigation, Resources, Writing, Pau Bosch-Jimenez: Supervision, Eduard Borràs: Resources.

References

[1] G. Fulli, M. Masera, A. Spisto, S. Vitiello, A change is coming: how regulation and innovation are reshaping the European Union's electricity markets, IEEE Power Energy Mag. 17 (2019) 53–66, https://doi.org/10.1109/MPE.2018.2872303 https://doi.org/.

[2] C.T. Pham, D. Månsson, Assessment of energy storage systems for power system applications via suitability index approach (Part IV), J. Energy Storage 24 (2019), https://doi.org/10.1016/j.est.2019.100777 https://doi.org/.

[3] P. Prabhakaran, D. Giannopoulos, W. Köppel, U. Mukherjee, G. Remesh, F. Graf, D. Trimis, T. Kolb, M. Founti, Cost optimisation and life cycle analysis of SOEC based Power to Gas systems used for seasonal energy storage in decentral systems, J. Energy Storage 26 (2019), https://doi.org/10.1016/j.est.2019.100987 https://doi.org/.

[4] A. Strbac, G. Aunedi, M. Pudjianto, D. Djapic, P. Teng, f. Sturt, Strategic assessment of the role and value of energy storage systems in the UK low carbon energy future report for, Carbon Trust (2012) 1–99.

[5] P. Denholm, E. Ela, B. Kirby, M. Milligan, Role of Energy Storage with Renewable Electricity Generation, (2010). https://doi.org/10.2172/972169.

[6] S. Hajiaghasi, A. Salemnia, M. Hamzeh, Hybrid energy storage system for microgrids applications: a review, J. Energy Storage 21 (2019) 543–570, https://doi.org/10.1016/j.est.2018.12.017 https://doi.org/.

[7] P. Ralon, M. Taylor, A. Ilas, H. Diaz-Bone, K.-P. Kairies, Electricity storage and renewables: Costs and markets to 2030, International Renewable Energy Agency (2017).

[8] B. Zakeri, S. Syri, Electrical energy storage systems: a comparative life cycle cost analysis, Renew. Sustain. Energy Rev. 42 (2015) 569–596, https://doi.org/10.1016/j.rser.2014.10.011 https://doi.org/.

[9] V.C. Patil, J. Liu, P.I. Ro, Efficiency improvement of liquid piston compressor using metal wire mesh for near-isothermal compressed air energy storage application, J. Energy Storage 28 (2020), https://doi.org/10.1016/j.est.2020.101226 https://doi.org/.

[10] H. Chen, H. Wang, R. Li, Y. Zhang, X. He, Thermo-dynamic and economic analysis of s a novel near- isothermal pumped hydro compressed air energy storage system, J. Energy Storage 30 (2020) 101487, , https://doi.org/10.1016/j.est.2020.101487 https://doi.org/.

[11] H. Blanco, A. Faaij, A review at the role of storage in energy systems with a focus on power to gas and long-term storage, Renew. Sustain. Energy Rev. 81 (2018) 1049–1086, https://doi.org/10.1016/j.rser.2017.07.062 https://doi.org/.

[12] Z. Yuan, S. He, A. Alizadeh, S. Nojavan, K. Jermsittiparsert, Probabilistic scheduling of power-to-gas storage system in renewable energy hub integrated with demand response program, J. Energy Storage 29 (2020), https://doi.org/10.1016/j.est.2020.101393 https://doi.org/.

[13] E. Kötter, L. Schneider, F. Sehnke, K. Ohnmeiss, R. Schröer, The future electric power system: impact of power-to-gas by interacting with other renewable energy components, J. Energy Storage 5 (2016) 113–119, https://doi.org/10.1016/j.est.2015.11.012 https://doi.org/.

[14] M. Bailera, P. Lisbona, L.M. Romeo, S. Espatolero, Power to Gas projects review: Lab, pilot and demo plants for storing renewable energy and CO_2, Renew. Sustain. Energy Rev. 69 (2017) 292–312, https://doi.org/10.1016/j.rser.2016.11.130 https://doi.org/.

[15] F.D. Meylan, F.P. Piguet, S. Erkman, Power-to-gas through CO_2 methanation: assessment of the carbon balance regarding EU directives, J. Energy Storage 11 (2017) 16–24, https://doi.org/10.1016/j.est.2016.12.005 https://doi.org/.

[16] B. Sheykhloei, T. Abedinzadeh, L. Mohammadian, B. Mohammadi-Ivatloo, Optimal co-scheduling of distributed generation resources and natural gas network considering uncertainties, J. Energy Storage 21 (2019) 383–392, https://doi.org/10.1016/j.est.2018.11.018 https://doi.org/.

[17] 2020 Gas Decarbonisation Pathways study - Gas for Climate 2050, (2020). https://gasforclimate2050.eu/sdm_downloads/2020-gas-decarbonisation-pathways-study/ (accessed May 23, 2020).

[18] M. Thema, T. Weidlich, M. Hörl, A. Bellack, F. Mörs, F. Hackl, M. Kohlmayer, J. Gleich, C. Stabenau, T. Trabold, M. Neubert, F. Ortlo, R. Brotsack, D. Schmack, H. Huber, D. Hafenbradl, J. Karl, M. Sterner, Biological CO_2-methanation: an approach to standardization, Energies 12 (2019) 1–32.

[19] X. Xing, J. Lin, Y. Song, Y. Zhou, S. Mu, Q. Hu, Modeling and operation of the power-to-gas system for renewables integration : a review, CSEE J. Power Energy Syst. 4 (2018) 168–178, https://doi.org/10.17775/CSEEJPES.2018.00260 https://doi.org/.

[20] M. David, C. Ocampo-Martínez, R. Sánchez-Peña, Advances in alkaline water electrolyzers: a review, J. Energy Storage 23 (2019) 392–403, https://doi.org/10.1016/j.est.2019.03.001 https://doi.org/.

[21] S. Schiebahn, T. Grube, M. Robinius, V. Tietze, B. Kumar, D. Stolten, Power to gas: technological overview, systems analysis and economic assessment for a case study in Germany, Int. J. Hydrog. Energy 40 (2015) 4285–4294, https://doi.org/10.1016/j.ijhydene.2015.01.123 https://doi.org/.

[22] Q. Li, Y. Zheng, W. Guan, L. Jin, C. Xu, W.G. Wang, Achieving high-efficiency hydrogen production using planar solid-oxide electrolysis stacks, Int. J. Hydrog. Energy 39 (2014) 10833–10842, https://doi.org/10.1016/j.ijhydene.2014.05.070 https://doi.org/.

[23] F. Geppert, D. Liu, M. van Eerten-Jansen, E. Weidner, C. Buisman, A. ter Heijne, Bioelectrochemical power-to-gas: state of the art and future perspectives, Trends Biotechnol 34 (2016) 879–894, https://doi.org/10.1016/j.tibtech.2016.08.010 https://doi.org/.

[24] R. Blasco-Gómez, P. Batlle-Vilanova, M. Villano, M.D. Balaguer, J. Colprim, S. Puig, On the edge of research and technological application: a critical review of electromethanogenesis, Int. J. Mol. Sci. 18 (2017) 1–32, https://doi.org/10.3390/ijms18040874 https://doi.org/.

[25] R.S. Muñoz-Aguilar, D. Molognoni, P. Bosch-Jimenez, E. Borràs, M. Della Pirriera, Á. Luna, Design, operation, modeling and grid integration of power-to-gas bioelectrochemical systems, Energies 11 (2018) 1–15, https://doi.org/10.3390/en11081947 https://doi.org/.

[26] A. Ceballos-Escalera, D. Molognoni, P. Bosch-Jimenez, M. Shahparasti, S. Bouchakour, A. Luna, A. Guisasola, E. Borràs, M. Della Pirriera, Bioelectrochemical systems for energy storage: a scaled-up power-to-gas approach, Appl. Energy (2019) 114138, , https://doi.org/10.1016/J.APENERGY.2019.114138 https://doi.org/.

[27] F. Enzmann, D. Holtmann, Rational scale-up of a methane producing bioelectrochemical reactor to 50 L pilot scale, Chem. Eng. Sci. 207 (2019) 1148–1158, https://doi.org/10.1016/J.CES.2019.07.051 https://doi.org/.

[28] M. Shahparasti, A. Luna, J. Rocabert, P. Bosch, P. Rodriguez, Realization of a 10 kW MES power to methane plant based on unified AC/DC converter, Proceedings of the 2018 IEEE Energy Conversion Congress and Exposition, ECCE, Portland, OR, 2018, pp. 3633–3640.

[29] Y. Zhang, Z. Mao, S. Cheng, M. Yu, W. Wei, X. Wu, Model Construction of the Electric Methane Generation Based on Biocatalyst, Institute of Electrical and Electronics Engineers (IEEE), 2020, pp. 126–131, https://doi.org/10.1109/ei247390.2019.9062096 https://doi.org/.

[30] M. Shahparasti, J. Rocabert, R.S. Muñoz, A. Luna, P. Rodríguez, Smart AC storage based on microbial electrosynthesis stack, Proceedings of the 7th International Conference on Renewable Energy Research and Applications, 2018, pp. 1086–1091.

[31] M. Shahparasti, J. Rocabert, R.S. Muñoz, A. Luna, P. Rodríguez, Impedance source interlinking converter for microbial electrosynthesis energy storage applications, Proceedings of the 7th International Conference on Renewable Energy Research and Applications, 2018, pp. 1340–1345.

[32] K. Marouani, K. Nounou, M. Benbouzid, B. Tabbache, Investigation of energy-efficiency improvement in an electrical drive system based on multi-winding machines, Electr. Eng. 100 (2018) 205–216, https://doi.org/10.1007/s00202-016-0493-z https://doi.org/.

[33] A.G. Capodaglio, D. Molognoni, A.V. Pons, A multi-perspective review of microbial fuel-cells for wastewater treatment: Bio-electro-chemical, microbiologic and modeling aspects, Proceedings of the 2016 AIP Conference Proceedings, American Institute of Physics Inc., 2016030032, , , https://doi.org/10.1063/1.4959428 https://doi.org/.

[34] D. Recio-garrido, M. Perrier, B. Tartakovsky, Modeling, optimization and control of bioelectrochemical systems, Chem. Eng. J. 289 (2015) 180–190, https://doi.org/10.1016/j.cej.2015.11.112 https://doi.org/.

[35] S.A. Hussain, M. Perrier, B. Tartakovsky, Real-time monitoring of a microbial electrolysis cell using an electrical equivalent circuit model, Bioprocess Biosyst. Eng. 41 (2018) 543–553, https://doi.org/10.1007/s00449-017-1889-5 https://doi.org/.

[36] F. Soavi, C. Santoro, Supercapacitive operational mode in microbial fuel cell, Curr. Opin. Electrochem. 22 (2020) 1–8, https://doi.org/10.1016/j.coelec.2020.03.009 https://doi.org/.

[37] N. Wagner, Characterization of membrane electrode assemblies in polymer electrolyte fuel cells using A.C. impedance spectroscopy, J. Appl. Electrochem. 32 (2002) 859–863, https://doi.org/10.1023/A:1020551609230 https://doi.org/.

[38] M. Sindhuja, N.S. Kumar, V. Sudha, S. Haripriya, Equivalent circuit modeling of microbial fuel cells using impedance spectroscopy, J. Energy Storage 7 (2016) 136–146, https://doi.org/10.1016/j.est.2016.06.005 https://doi.org/.

[39] R.P. Ramasamy, Z. Ren, M.M. Mench, J.M. Regan, Impact of initial biofilm growth on the anode impedance of microbial fuel cells, Biotechnol. Bioeng. 101 (2008) 101–108, https://doi.org/10.1002/bit.21878 https://doi.org/.

[40] Z. He, N. Wagner, S.D. Minteer, L.T. Angenent, An upflow microbial fuel cell with an interior cathode: assessment of the internal resistance by impedance spectroscopy †, Environ. Sci. Technol. 40 (2006) 5212–5217, https://doi.org/10.1021/es060394f https://doi.org/.

[41] J. Do Park, T.M. Roane, Z.J. Ren, M. Alaraj, Dynamic modeling of a microbial fuel cell considering anodic electron flow and electrical charge storage, Appl. Energy. 193 (2017) 507–514, https://doi.org/10.1016/j.apenergy.2017.02.055 https://doi.org/.

[42] S.A. Hussain, Dynamic Modeling and Intermittent Operation of a Flow-Through Microbial Electrolysis Cell, École Polytechnique De Montréal, 2018.

[43] C. Santoro, C. Arbizzani, B. Erable, I. Ioannis, Microbial fuel cells: from fundamentals to applications. A review, J. Power Sour. 356 (2017) 225–244, https://doi.org/10.1016/J.JPOWSOUR.2017.03.109 https://doi.org/.